An asymptotic theory of incompressible turbulent boundary-layer flow over a small hump

By R. I. SYKES†

Meteorological Office, Bracknell, Berkshire

A rational asymptotic theory describing the perturbed flow in a turbulent boundary layer encountering a small two-dimensional hump is presented. The theory is valid in the limit of very high Reynolds number in the case of an aerodynamically smooth surface, or in the limit of small drag coefficient in the case of a rough surface. The method of matched asymptotic expansions is used to obtain a multiple-structured flow, along the general lines of earlier laminar studies. The leading-order velocity perturbations are shown to be precisely the inviscid, irrotational, potential flow solutions over most of the domain. The Reynolds stresses are found to vary across a thin layer adjacent to the surface, and display a singular behaviour near the surface which needs to be resolved by an even thinner wall layer. The Reynolds stress perturbations are calculated by means of a second-order closure model, which is shown to be the minimum level of sophistication capable of describing these variations. The perturbation force on the hump is also calculated, and its order of magnitude is shown to depend on the level of turbulence closure; a cruder turbulence model gives rise to spuriously large forces.

1. Introduction

An understanding of boundary-layer flow over surface-mounted obstacles has many applications in aerodynamics and meterology. A number of recent studies have been directed at the problem, and much progress has been made for the laminar-flow case. However, the dynamics of the turbulent problem are not so well understood, although most boundary layers of practical interest are in fact turbulent. The aim of the present work is the development of a rational asymptotic theory of incompressible turbulent flow over a shallow hump, which will hopefully elucidate the dynamics involved.

The laminar problem for asymptotically large Reynolds number was first investigated by Hunt (1971), and later by Smith (1973), Smith, Sykes & Brighton (1977) and Sykes (1978) using 'triple-deck' theory. This is a three-layer structure using matched asymptotic expansions, reviewed by Stewartson (1974), and is more general than the earlier two-layer, locally-valid structure of Hunt (1971). The predictions of the triple-deck theory have been confirmed at moderate Reynolds number by means of comparisons with numerical integrations of the Navier–Stokes equation by Mason & Sykes (1979a).

Townsend (1972) presents a linearized analysis of turbulent flow over a wavy surface using a turbulence closure of the type proposed by Bradshaw, Ferriss & Atwell (1967).

† Present address: Aeronautical Research Associates of Princeton, 50 Washington Road, Princeton, New Jersey 08540, U.S.A.

This is not an asymptotic theory in a strict sense, but simplifies the equations by the neglect of various small terms. The main concern is with travelling surface waves, but some results are presented for the case of a stationary wave. Knight (1977) gives some of the leading-order terms in an asymptotic solution to the travelling-wave problem, and there is some agreement between his work and the theory presented here; unfortunately his paper does not contain sufficient detail to make useful comparisons. Several numerical solutions of the equations for turbulent boundary-layer flow over topography under simple closure assumptions have been obtained (see, for example, Taylor & Gent 1975; Deaves 1975; Taylor 1977). Although these studies reveal the main features of the flow, an asymptotic study can still contribute significantly to our understanding of the dynamics. Counihan, Hunt & Jackson (1974) give a theory of the far-field turbulent wake behind a small bluff obstacle; the flow structure is composed of layers of different asymptotic scales, but the perturbations are not expanded as a rational series in a small parameter. This makes the solutions rather specific to the problem under consideration, and the details of the dynamics are obscured by the non-rigorous expansion procedure. Furthermore, the authors were not able to obtain a smooth match with the wall layer on the lower boundary.

A linear analysis of the flow over a gentle hump is given by Jackson & Hunt (1975). This analysis considers two layers; an outer inviscid layer; and an inner region where the turbulent Reynolds stresses are parameterized by means of a mixing length closure. There are some problems with matching the solutions again in this theory, but these will be discussed further below. One aspect of the problem of flow over a hump which Jackson & Hunt do not address is the question of the change in total force on the solid boundary due to the presence of the obstacle. In view of the laminar boundary-layer force results of Sykes (1978) and Mason & Sykes (1979a), which show that the reduction in surface stress in the wake can largely balance the pressure force on a small obstacle, it is not obvious what magnitude the total force perturbation will have in the turbulent case. The perturbation force requires higher-order terms in the expansions to be calculated, and the difficulty with the calculation of such terms in the theory of Jackson & Hunt (1975) was one of the motivations for the development of a rational asymptotic theory.

Recent work on turbulent boundary layer shock wave interactions by Adamson & Feo (1975) and Melnik & Grossman (1974) has shown that asymptotic flow structures of the same general form as the laminar triple-deck, but very different in detail and dynamics, can be constructed for turbulent flow. The theory presented below is essentially an extension of the turbulent trailing-edge flow developed by Melnik & Chow 1975 to the case of a gentle hump lying within a boundary layer.

The theory has a three-layer structure in the vertical, although the innermost layer is extremely thin, and plays little direct part in the dynamics other than providing the match with the lower boundary condition. The analysis is presented using a horizontal length scale of the same order as the boundary layer depth, as in Melnik & Chow (1975); however it will be shown that the same structure applies over a wide range of length scales. It is shown that the mixing length hypothesis, which assumes local equilibrium for the turbulence, is inadequate for the intermediate layer, and a second-order closure turbulence model of the type described by Hanjalic & Launder (1972) is employed. This provides information on turbulence moments in addition to mean velocity fields. The rational expansion procedure also allows the calculation of higher order terms, and
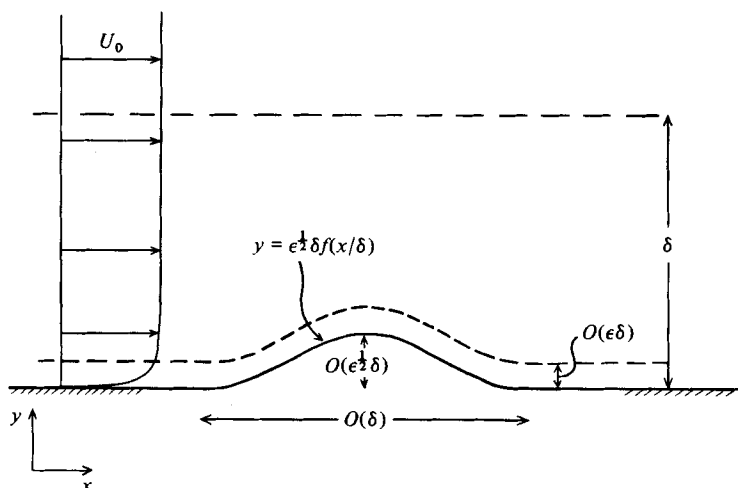
FIGURE 1. Schematic illustration of flow geometry.

the total force is derived and shown to be non-zero. Consideration of the effects of other closure assumptions shows that the perturbation force on the surface has different orders of magnitude for different levels of closure.

The turbulent flow to be described is very much less interactive than the laminar triple-deck, mainly due to the small shear in the turbulent boundary layer. To leading order, the velocity perturbations are simply given by linearized potential flow, and the most interesting new results are the Reynolds-stress perturbations. These show a very rapid adjustment from the equilibrium wall layer values to the outer part of the stress field which is strongly influenced by its upstream history.

The perturbations are all linearized, and the theory is unable to deal with strong perturbations; unlike the triple-deck which is a nonlinear theory capable of describing separation. In fact, this work suggests that slopes of order unity are necessary to provoke separation; this conclusion is supported by the work of Adamson & Feo (1975) and Melnik & Grossman (1974).

2. Flow structure and equations of motion

Consider a turbulent boundary layer of thickness δ developed over a rigid lower boundary, with external flow speed U_0, as depicted in figure 1. The boundary layer is characterized by the small parameter $\epsilon = u_*/U_0$, where $u_*^2 = \tau_0$ is the stress on the flat boundary in the absence of topography. We shall consider variations in surface elevation of order $\epsilon^{\frac{1}{2}}\delta$ on a horizontal length scale of order δ.

The application of asymptotic methods to the problem of an incompressible turbulent boundary layer on a smooth wall, for example, Yajnik (1970), Mellor (1972), has led to a systematic two-layer description of the flow. This consists of an outer defect layer on the scale of the boundary layer where the velocity magnitude only differs from the free-stream speed by an amount of $O(\epsilon)$, and has a logarithmic variation as the boundary is approached. This matches with the logarithmic wall layer defined in terms of the variable $y^+ = \bar{y}u_*/\nu$, where $\bar{y}$ is the distance from the wall and ν the

kinematic viscosity. Thus the wall layer has a thickness of $O(\epsilon^{-1}R^{-1})$ where $R = U_0\delta/\nu$ is the Reynolds number based on the boundary layer thickness. Hence, the upstream velocity profiles required for the present work are taken to be

$$u(\bar{y})/U_0 = 1 + \epsilon u_{BL}(y) \tag{2.1}$$

in the outer defect layer, where $y = \bar{y}/\delta$ and

$$u_{BL}(y) = \begin{cases} \dfrac{1}{\kappa}\ln y - \dfrac{\hat{\pi}_T}{\kappa}W(y), & y \leqslant 1, \\ 0 & y > 1. \end{cases} \tag{2.2}$$

Here $\hat{\pi}_T$ is the Coles wake parameter, κ is von Kármán's constant, and $W(y)$ is the wake function (see, for example, Coles 1956; Hinze 1959). Note that although the mean velocity is constant to $O(\epsilon)$ on the scale δ the Reynolds stresses vary on this length scale so that the definition of the boundary-layer depth is meaningful.

The wall-layer profile is assumed to satisfy

$$\frac{u(\bar{y})}{U_0} \sim \epsilon\left(\frac{1}{\kappa}\ln y^+ + B\right) \quad \text{as} \quad y^+ \to \infty. \tag{2.3}$$

In fact, we shall only require that the wall layer be transcendentally thin compared to the boundary-layer scale, and make use of the asymptotically logarithmic variation of velocity. Thus the aerodynamically rough wall can also be included in the analysis if we consider the wall layer to have thickness y_0, where y_0 is the roughness length which is defined from the near-wall form of the velocity profile, i.e.

$$\frac{u(\bar{y})}{U_0} \sim \frac{\epsilon}{\kappa}\ln\frac{\bar{y}}{y_0} \quad \text{as} \quad \frac{\bar{y}}{\delta} \to 0. \tag{2.4}$$

Therefore, defining $y^+ = \bar{y}/y_0$, the rough wall has the same behaviour as the smooth wall, since the constant B in (2.3) can be absorbed into the definition of y^+.

Following Melnik & Chow (1975), we shall consider a dimensionless perturbation of $O(\epsilon^{\frac{1}{2}})$, which will be produced by a hump of height $O(\epsilon^{\frac{1}{2}}\delta)$. We shall show that in the main part of the boundary layer, the Reynolds stresses are subjected to a rapid distortion, whilst the stresses in the wall layer are always in equilibrium with the surface. An intermediate layer is required to provide a smooth transition between the two Reynolds-stress values. This region turns out to have a thickness $O(\epsilon\delta)$, i.e. smaller than the height of the obstacle, and is thus a thin layer attached to the curved surface. This structure is illustrated schematically in figure 1.

As mentioned previously, it will be shown that the Reynolds stresses in the outer layer are rapidly distorted. This implies that a simple mixing length or so-called 'first-order' turbulence closure assumption is inadequate for a description of the entire flow. A more sophisticated closure scheme is necessary, but we postpone discussion of our choice of closure until the next section. We now present the expansions and the equations for the velocity field.

Outer layer

The undisturbed velocity profile is given by (2.1) and (2.2) where $y = \bar{y}/\delta$ is the dimensionless normal co-ordinate in the outer layer. Scaling the streamwise co-ordinate, x by δ, we expand the velocity and pressure as follows

$$\left.\begin{aligned}
\frac{u}{U_0} &= 1 + \epsilon^{\frac{1}{2}} u_1(x,y) + \epsilon(u_{BL}(y - \epsilon^{\frac{1}{2}} f(x)) + u_2(x,y)) + \epsilon^{\frac{3}{2}} u_3(x,y) + \dots, \\
\frac{v}{U_0} &= \epsilon^{\frac{1}{2}} v_1(x,y) + \epsilon v_2(x,y) + \epsilon^{\frac{3}{2}} v_3(x,y) + \dots, \\
\frac{p}{\rho U_0^2} &= \epsilon^{\frac{1}{2}} p_1(x,y) + \epsilon p_2(x,y) + \epsilon^{\frac{3}{2}} p_3(x,y) + \dots,
\end{aligned}\right\} \tag{2.5}$$

where ρ is the density of fluid, and $y = \epsilon^{\frac{1}{2}} f(x)$ is the profile of the lower surface, i.e. the upstream profile u_{BL} is displaced over the obstacle.

The basic Reynolds stresses are $O(\epsilon^2 U_0^2)$, and since the perturbation stresses are $O(\epsilon^{\frac{3}{2}} U_0^2)$, the outer flow is inviscid up to $O(\epsilon^{\frac{3}{2}})$. Thus, the two leading-order terms are simply the first two terms of linearized potential flow, i.e.

$$\frac{\partial u_1}{\partial x} = -\frac{\partial p_1}{\partial x}, \quad \frac{\partial v_1}{\partial x} = -\frac{\partial p_1}{\partial y}, \quad \frac{\partial u_1}{\partial x} + \frac{\partial v_1}{\partial y} = 0, \tag{2.6}$$

and

$$\left.\begin{aligned}
\frac{\partial u_2}{\partial x} + u_1 \frac{\partial u_1}{\partial x} + v_1 \frac{\partial u_1}{\partial y} &= -\frac{\partial p_2}{\partial x}, \\
\frac{\partial v_2}{\partial x} + u_1 \frac{\partial v_1}{\partial x} + v_1 \frac{\partial v_1}{\partial y} &= -\frac{\partial p_2}{\partial y}, \\
\frac{\partial u_2}{\partial x} + \frac{\partial v_2}{\partial y} &= 0.
\end{aligned}\right\} \tag{2.7}$$

Hence

$$\nabla^2 p_1 = 0 \tag{2.8}$$

and

$$\nabla^2 p_2' = 0 \tag{2.9}$$

where $p_2' = p_2 + \frac{1}{2}(u_1^2 + v_1^2)$, and we have used the fact that $\partial u_1/\partial y = \partial v_1/\partial x$, i.e. the flow is irrotational. Higher-order terms will involve the rotational boundary-layer component, $u_{BL}(y - \epsilon^{\frac{1}{2}} f(x))$.

The lower boundary conditions on the outer flow equations must come from matching with the inner layers.

Wall layer

We consider next the wall layer of thickness y_0, or $\epsilon^{-1} R^{-1} \delta$. We define the wall-layer variable $y^+ = (\bar{y} - \epsilon^{\frac{1}{2}} \delta f(x))/y_0$. Since we have the relation $\epsilon \ln \delta/y_0 = O(1)$ (or $\epsilon \ln \epsilon R = O(1)$) from the requirement that the asymptotic wall-layer profile (2.4) (or (2.3)) must match with the outer-layer profile (2.1), the wall layer is transcendentally thin. Thus the total stress gradient, i.e. Reynolds stress plus viscous stress in the smooth wall case, is zero to all orders across the wall layer.

Using the asymptotic form (2.4), the wall-layer condition is

$$\frac{u_t}{U_0} \sim \frac{\epsilon}{\kappa} (\tau_w^+(x))^{\frac{1}{2}} \ln y^+ \quad \text{as} \quad y^+ \to \infty \tag{2.10}$$

where τ_w^+ is the dimensionless stress on the boundary, and u_t is the velocity component tangential to the surface.

We expand τ_w^+ as follows:

$$\tau_w^+ = 1 + \epsilon^{\frac{1}{2}}\tau_1^+(x) + \epsilon\tau_2^+(x) + \epsilon^{\frac{3}{2}}\ln\epsilon\tau_{31}^+(x) + \epsilon^{\frac{3}{2}}\tau_3^+(x) + \ldots, \tag{2.11}$$

where the logarithmic terms are generated by the match with the Reynolds-stress sublayer.

Reynolds-stress sublayer

The normal co-ordinate in this layer is taken to be $Y = (\bar{y} - \epsilon^{\frac{1}{2}}\delta f(x))/\epsilon\delta$, and we expand

$$\left.\begin{aligned}
\frac{u}{U_0} &= 1 + \epsilon^{\frac{1}{2}}U_1(x, Y) + \frac{\epsilon\ln\epsilon}{\kappa} + \epsilon(U_{BL}(Y) + U_2) + \epsilon^{\frac{3}{2}}\ln\epsilon\, U_{31} + \epsilon^{\frac{3}{2}}U_3 + \ldots, \\
\frac{p}{\rho U_0^2} &= \epsilon^{\frac{1}{2}}P_1(x, Y) + \epsilon P_2 + \epsilon^{\frac{3}{2}}\ln\epsilon P_{31} + \epsilon P_3 \ldots,
\end{aligned}\right\} \tag{2.12}$$

where
$$U_{BL}(Y) = \frac{1}{\kappa}\ln Y - 2\bar{\pi}_T.$$

If we define

$$v = \epsilon^{\frac{1}{2}}u\frac{df}{dx} + v^* \tag{2.13}$$

then

$$\left.\frac{\partial u}{\partial x}\right|_Y + \epsilon^{-1}\frac{\partial v^*}{\partial Y} = 0, \tag{2.14}$$

and we expand

$$\frac{v^*}{U_0} = \epsilon^{\frac{3}{2}}V_1^*(x, Y) + \epsilon_2 V_2^* + \epsilon^{\frac{5}{2}}\ln\epsilon V_{31}^* + \epsilon^{\frac{5}{2}}V_3^* + \ldots. \tag{2.15}$$

Finally, the Reynolds stresses $\tau_{ij} = -\overline{u_i' u_j'}$ are expanded as follows

$$\frac{\tau_{ij}}{U_0^2} = \epsilon^2 A_{ij} + \epsilon^{\frac{5}{2}}T_{ij}^{(1)}(x, Y) + \epsilon^2 T_{ij}^{(2)} + \ldots, \tag{2.16}$$

where A_{ij} is the dimensionless equilibrium Reynolds-stress tensor near the surface in the undisturbed flow; A_{ij} is a constant tensor because the Reynolds stress varies on the scale δ in the upstream boundary layer. We also know that $A_{12} = 1$, and the only other non-zero components are the diagonal terms, which are all negative.

Substituting the expansions (2.12), (2.15), (2.16) into the Reynolds-averaged Navier–Stokes equations, and remembering the non-orthogonal co-ordinate system, we obtain a sequence of perturbation equations. The $O(\epsilon^{\frac{1}{2}})$ terms give

$$\frac{\partial U_1}{\partial x} = -\frac{\partial P_1}{\partial x}, \quad \frac{\partial P_1}{\partial Y} = 0$$

where $\partial/\partial x$ indicates $\partial/\partial x|_Y$.

Thus

$$U_1(x) = u_1(x, 0), \quad P_1(x) = p_1(x, 0),$$
$$V_1^*(x, Y) = -Y\frac{dU_1}{dx} \Bigg\}$$

(2.17)

since the velocity and pressure must match with the outer flow.

At $O(\epsilon)$, we have

$$\frac{\partial U_2}{\partial x} + U_1\frac{\partial U_1}{\partial x} = -\frac{\partial P_2}{\partial x} - f'f'', \quad \frac{\partial P_2}{\partial Y} = 0$$

where we have used the $O(\epsilon^{\frac{3}{2}})$ result that

$$\frac{\partial P_3}{\partial Y} = -f''.$$

The prime denotes differentiation with respect to x.

Thus

$$P_2(x) = p_2(x, 0) + f\frac{\partial p_1}{\partial y}\Bigg|_0,$$
$$U_2(x) = u_2(x, 0) + f\frac{\partial u_1}{\partial y}\Bigg|_0,$$
$$V_1^*(x, Y) = -Y\frac{dU_2}{dx}. \Bigg\}$$

(2.18)

At $O(\epsilon^{\frac{3}{2}}\ln\epsilon)$:

$$\frac{\partial U_{31}}{\partial x} + \frac{1}{\kappa}\frac{dU_1}{dx} = -\frac{\partial P_{31}}{\partial x}, \quad \frac{\partial P_{31}}{\partial Y} = 0.$$

From the match with the outer flow

$$P_{31} = 0, \quad U_{31} = \frac{1}{\kappa}U_1(x).$$

(2.19)

The $O(\epsilon^{\frac{3}{2}})$ terms give

$$\frac{\partial U_3}{\partial x} = -\frac{\partial P_3}{\partial x} - 2U_1f'f'' + \frac{\partial T_{12}^{(1)}}{\partial Y} - \frac{d}{dx}(U_1U_2) - U_{BL}\frac{dU_1}{dx} - V_1^*\frac{dU_{BL}}{dY},$$
$$\frac{\partial P_3}{\partial Y} = -f''. \Bigg\}$$

(2.20)

The Reynolds-stress perturbation, $T_{ij}^{(1)}$, has made its appearance at this order, and therefore some closure scheme is required before equations (2.20) can be solved. We postpone discussion of the turbulence closure until the next section, and consider now the lower-order solutions which are independent of any closure assumptions.

Leading-order solutions

The outer flow solution to lowest order is potential flow, equations (2.6) and (2.8), and the match with the inner layer (2.13), (2.15) gives the lower boundary condition

$$v_1(x, 0) = df/dx.$$

(2.21)

Thus

$$\nabla^2 p_1 = 0$$

and

$$\frac{\partial p_1}{\partial y} = -f'' \quad \text{on} \quad y = 0. \Bigg\}$$

(2.22)

Similarly, at $O(\epsilon)$,

$$\nabla^2 p_2' = 0,$$

and

$$\frac{\partial p_2'}{\partial y} = -\frac{d}{dx}\left(U_1 \frac{df}{dx}\right) \quad \text{on} \quad y = 0 \Bigg\}$$

(2.23)

where p_2' is defined immediately after (2.9).

Hence the two lowest-order terms are simply the linearized inviscid potential flow terms for flow over the perturbed lower boundary. The corresponding terms in the inner Reynolds-stress sublayer are obtained by matching with these, and are just the potential flow solution values at the lower boundary $y = \epsilon^{\frac{3}{2}} f(x)$, as can be seen from (2.17) and (2.18).

Having obtained the leading-order terms, it is possible to deduce the form of the Reynolds stresses near the surface. First, in the wall layer, the stresses are independent of distance from the surface, and the velocity is given by the logarithmic profile (2.10). From (2.11),

$$\sqrt{\tau_w^+} = 1 + \tfrac{1}{2} \epsilon^{\frac{1}{2}} \tau_1^+ + \epsilon \left(\frac{\tau_2^+}{2} - \frac{\tau_1^{+2}}{8}\right) + \dots .$$

(2.24)

The matching of the boundary layer profiles requires $(\epsilon/\kappa) \ln(\delta/y_0) = 1 - 2\hat{\pi}_T \epsilon$, which can be regarded as fixing δ. Then rewriting (2.10) in terms of the Reynolds-stress sublayer variable Y,

$$\frac{u_t}{U_0} \sim \frac{\epsilon}{\kappa} \left\{ 1 + \tfrac{1}{2} \epsilon^{\frac{1}{2}} \tau_1^+ + \epsilon \left(\frac{\tau_2^+}{2} - \frac{\tau_1^{+1}}{8}\right) + \dots \right\} \left[\ln Y + \ln \epsilon + \ln \frac{\delta}{y_0} \right].$$

(2.25)

Before we can match with the Reynolds-stress sublayer, we have to account for the fact that the velocity is parallel to the surface in the wall layer. Thus the velocity in (2.25) must be multiplied by $\cos \theta$, where $\tan \theta = f'$. The final match with the Reynolds-stress sublayer is obtained as

$$\frac{u}{U_0} \sim 1 + \tfrac{1}{2} \epsilon^{\frac{1}{2}} \tau_1^+ + \frac{\epsilon \ln \epsilon}{\kappa} + \epsilon \left(\frac{\tau_2^+}{2} - \frac{\tau_1^{+2}}{8} - \frac{f'^2}{2} + \frac{1}{\kappa} \ln Y - 2\hat{\pi}_T\right) + \dots .$$

(2.26)

Thus

$$\tau_1^+ = 2U_1(x), \quad \tau_2^+ = 2U_2(x) + U_1^2 + f'^2.$$

(2.27)

These surface stress solutions will be used to provide a lower boundary condition for the Reynolds stresses in the Reynolds-stress sublayer in the next section. Before proceeding, there is a further feature of the Reynolds stress behaviour near the surface which can be deduced from (2.20). From (2.25), we see that there is a logarithmic term in the velocity at $O(\epsilon^{\frac{3}{2}})$, i.e.

$$U_3 \sim \frac{U_1}{\kappa} \ln Y + O(1) \quad \text{as} \quad Y \to 0.$$

Thus, remembering that $V_1^* = -Y dU_1/dx$, and using the definition of $U_{\mathrm{BL}}(Y)$, the balance of terms in (2.20) as $Y \to 0$ must include the stress-gradient term, in fact,

$$\frac{\partial T_{12}^{(1)}}{\partial Y} \sim \frac{2}{\kappa} \frac{dU_1}{dx} \ln Y \quad \text{as} \quad Y \to 0. \tag{2.28}$$

Hence the first-order stress gradient has a logarithmic singularity at the surface, whilst the Reynolds stresses themselves vary like $Y \ln Y$. This does not prevent a match with the zero-gradient condition in the wall layer, since the depth of the wall layer is transcendentally small. This singular behaviour of the Reynolds stress is independent of any closure assumption, and is obtained by Adamson & Feo (1975) using a mixing length closure. Counihan *et al.* (1974) also find a singular behaviour in the stresses near the surface, but they do not produce an asymptotic match with the wall layer. The rapid stress variation appears to be produced by the horizontal variations of velocity, and could well be a general feature of perturbed turbulent boundary layers.

3. Turbulence closure equations

The Reynolds-averaged equations for the components of the Reynolds-stress tensor are obtainable from the Navier–Stokes equations as

$$\overline{U}_k \frac{\partial}{\partial x_k} \overline{u_i u_j} = P_{ij} + D_{ij} + S_{ij}, \tag{3.1}$$

where $\overline{U}_i$ is the mean velocity, $\overline{u_i u_j}$ is the Reynolds stress and

$$P_{ij} = -\overline{u_i u_k} \frac{\partial \overline{U}_j}{\partial x_k} - \overline{u_k u_j} \frac{\partial \overline{U}_i}{\partial x_k},$$

$$D_{ij} = \nu \overline{\frac{\partial u_i}{\partial x_k} \frac{\partial u_j}{\partial x_k}},$$

$$S_{ij} = -\frac{\partial}{dx_k} \overline{(u_i u_j u_k)} - \frac{\partial}{\partial x_i} \overline{pu_j} - \frac{\partial}{\partial x_j} \overline{pu_i}.$$

Lower-case latters denote a fluctuating quantity. The tensor P_{ij} denotes the production terms, D_{ij} the dissipation and S_{ij} the third-order correlations.

Although (3.1) is not useful as a predictive equation, since D_{ij} and S_{ij} are unspecified, some idea of the orders of magnitude of the various terms can be inferred. Using the expansion (2.16) for the Reynolds stress, the mean-flow transport term on the left-hand side of (3.1) is $O(\epsilon^{\frac{5}{2}} U_0^3 \delta^{-1})$ in both the outer flow and the Reynolds-stress sublayer. The perturbation production terms in both layers are also $O(\epsilon^{\frac{5}{2}} U_0^3 \delta^{-1})$, as can be seen by substituting the leading orders for the velocity gradients in the definition of P_{ij}. The undisturbed third-order correlation $\overline{u_i u_j u_k}$ is $O(\epsilon^3 U_0^3)$, therefore the perturbation will be $O(\epsilon^{\frac{7}{2}} U_0^3)$. This term represents the turbulent transport of the Reynolds stresses, and therefore in the outer layer the turbulent diffusion is $O(\epsilon^{\frac{7}{2}} U_0^3 \delta^{-1})$ and in the Reynolds-stress sublayer it is $O(\epsilon^{\frac{5}{2}} U_0^3 \delta^{-1})$. We have considered only the three basic terms in equation (3.1) in order to assess the important mechanisms; the remaining terms do not contribute different orders of magnitude to the analysis. From this crude

analysis, it will be seen that diffusion is negligible in the outer layer, but is the same order as the other terms in the Reynolds-stress sublayer. This confirms the role of the Reynolds-stress sublayer as a blending layer between the wall layer, where the stresses are in local equilibrium, and the outer flow, where the stresses are rapidly distorted. It also prohibits any simple turbulence closure scheme, since the solutions must encompass both the mixing-length result near the surface and the rapid-distortion result at the outer edge. This conclusion is also reached by Britter, Hunt & Richards (1980), where the 'rapid-distortion' theory of Batchelor & Proudman (1954) is used to calculate the turbulence changes in the outer flow.

The closure scheme which we shall adopt is the so-called 'second-order' closure proposed by Donaldson (1971), and developed by Hanjalic & Launder (1972), and Launder, Reece & Rodi (1975). In order not to complicate unduly the equations, we shall not use the 'wall terms' of Launder *et al.* (1975), but we shall use the simplified model of the rapid pressure terms which they suggest. We also use the simplified model of the turbulent diffusion terms. Irwin & Smith (1975) have shown that this type of model accounts for the effects of streamline curvature on the Reynolds stresses, and we therefore have some confidence that the predictions for the problem under consideration will be useful. The modelled terms we shall use are

$$S_{ij} = c_s' \frac{\partial}{\partial x_l} \left(\frac{\overline{qu_k u_l}}{D} \frac{\partial}{\partial x_k} \overline{u_i u_j} \right) - c_1 \frac{D}{q} (\overline{u_i u_j} - \tfrac{2}{3} q \delta_{ij}) - \gamma (P_{ij} - \tfrac{2}{3} P \delta_{ij}) \qquad (3.2)$$

where $q = \tfrac{1}{2} \overline{u_i u_j}$ is the turbulence energy, $P = \tfrac{1}{2} P_{ii}$ and δ_{ij} is the Kronecker delta; $D_{ij} = -\tfrac{2}{3} D \delta_{ij}$ is the dissipation which is assumed to be isotropic. c_1, c_s' and γ are empirical constants with the values recommended by Launder *et al.* (1975), namely 1·5, 0·25, 0·6 respectively. The first term in (3.2) is the turbulent diffusion, the second is the return-to-isotropy term due to Rotta (1951), and the third is the 'rapid' part of the pressure correlation. We still need to specify D in order to close the equations, and this is achieved by means of another transport equation as in Hanjalic & Launder (1972), i.e.

$$\overline{U}_k \frac{\partial D}{\partial x_k} = c_\epsilon \frac{D}{q} P + c_{\epsilon 1} \frac{\partial}{\partial x_k} \left(\frac{q}{D} \frac{\partial D}{\partial x_k} \right) - c_{\epsilon 2} \frac{D^2}{q} \qquad (3.3)$$

where $c_{\epsilon 1} = 1·45$, $c_\epsilon = 0·13$, $c_{\epsilon 2} = 2$.

This completes the closure of the Reynolds-stress equation, and we can now substitute the perturbation expansions (2.16), (2.12), and (2.15) into (3.1), (3.2), (3.3) to obtain the solution in the Reynolds-stress sublayer. We also need an expansion for D which we now make:

$$D = \frac{\epsilon^2 U_0^3}{\delta} \left\{ \frac{1}{\kappa Y} + \epsilon^{\frac{1}{2}} D_1(x, Y) + \dots \right\}. \qquad (3.4)$$

The first-order equations (with Cartesian x derivatives) are

$$\frac{\partial T_{11}^{(1)}}{\partial x} = -(1 - \gamma) P_{11} - \tfrac{2}{3} \gamma P - \frac{c_1}{\kappa q_0 Y} (T_{11}^{(1)} + \tfrac{2}{3} q_1) + \tfrac{2}{3} D_1$$

$$+ \frac{c_1}{\kappa q_0 Y} \left(\kappa Y D_1 - \frac{q_1}{q_0} \right) (A_{11} + \tfrac{2}{3} q_0) - c_s' \frac{\partial}{\partial Y} \left(\kappa q_0 Y A_{22} \frac{\partial T_{11}^{(1)}}{\partial Y} \right), \qquad (3.5)$$

$$\frac{\partial T_{22}^{(1)}}{\partial x} = -(1-\gamma)\,P_{22} - \tfrac{2}{3}\gamma P - \frac{c_1}{\kappa q_0\,Y}\,(T_{22}^{(1)} + \tfrac{2}{3}q_1) + \tfrac{2}{3}D_1$$
$$- \frac{c_1}{\kappa q_0\,Y}\left(\kappa YD_1 - \frac{q_1}{q_0}\right)(A_{22} + \tfrac{2}{3}q_0) - c_s'\frac{\partial}{\partial Y}\left(\kappa q_0\,YA_{22}\frac{\partial T_{22}^{(1)}}{\partial Y}\right), \quad (3.6)$$

$$\frac{\partial T_{33}^{(1)}}{\partial x} = -\tfrac{2}{3}\gamma P - \frac{c_1}{\kappa q_0\,Y}\,(T_{33}^{(1)} + \tfrac{2}{3}q_1) + \tfrac{2}{3}D_1$$
$$- \frac{c_1}{\kappa q_0\,Y}\left(\kappa YD_1 - \frac{q_1}{q_0}\right)(A_{33} + \tfrac{2}{3}q_0) - c_s'\frac{\partial}{\partial Y}\left(\kappa q_0\,YA_{22}\frac{\partial T_{33}^{(1)}}{\partial Y}\right), \quad (3.7)$$

$$\frac{\partial T_{12}^{(1)}}{\partial x} = -(1-\gamma)\,P_{12} - \frac{c_1}{\kappa q_0\,Y}\,T_{12}^{(1)} - \frac{c_1}{\kappa q_0\,Y}\left(\kappa YD_1 - \frac{q_1}{q_0}\right)$$
$$- c_s'\frac{\partial}{\partial Y}\left(\kappa q_0\,YA_{22}\frac{\partial T_{12}^{(1)}}{\partial Y}\right), \quad (3.8)$$

$$\frac{\partial D_1}{\partial x} = \frac{c_{\epsilon 1}}{\kappa q_0\,Y}\,P + \frac{c_{\epsilon 1}}{\kappa^2 q_0\,Y^2}\left(\kappa YD_1 - \frac{q_1}{q_0}\right) - c_{\epsilon 2}\left(2\kappa YD_1 - \frac{q_1}{q_0}\right) - c_\epsilon\frac{\partial}{\partial Y}\left(\kappa q_0\,YA_{22}\frac{\partial D_1}{\partial Y}\right)$$
$$- c_\epsilon\left\{\frac{A_{22}}{Y}\frac{\partial q_1}{\partial Y} + \frac{A_{22}q_1}{Y^2} + A_{22}\kappa q_0\frac{\partial D_1}{\partial Y} + \frac{q_0}{Y}\frac{\partial T_{33}^{(1)}}{\partial Y} - \frac{q_0 T_{33}^{(1)}}{Y^2}\right\} + \frac{V_1^*}{\kappa Y^2} + \frac{2c_\epsilon q_0}{Y^2}f'. \quad (3.9)$$

In the above equations

$$q_0 = -\tfrac{1}{2}(A_{11} + A_{22} + A_{33}),$$

$$q_1 = -\tfrac{1}{2}(T_{11}^{(1)} + T_{22}^{(1)} + T_{33}^{(1)}),$$

$$P_{11} = 2\left\{A_{11}\left(\frac{dU_1}{dx} - \frac{f'}{\kappa Y}\right) + \frac{\partial U_3}{\partial Y} + \frac{1}{\kappa Y}\,T_{12}^{(1)}\right\},$$

$$P_{22} = 2\left\{f'' - A_{22}\left(\frac{dU_1}{dx} - \frac{f'}{\kappa Y}\right)\right\},$$

$$P_{12} = A_{11}f'' + A_{22}\frac{\partial U_3}{\partial Y} + \frac{T_{22}^{(1)}}{\kappa Y}$$

and
$$P = \tfrac{1}{2}(P_{11} + P_{22}).$$

The upper boundary conditions on equations (3.5)–(3.9) are obtained by letting $Y \to \infty$. This leaves only the production terms and the 'rapid' pressure terms on the right-hand side, and the equations are easily solved, giving

$$\left.\begin{aligned}
T_{11}^{(1)} &\sim -\{2(1-\gamma)\,A_{11} + \tfrac{2}{3}\gamma(A_{11} - A_{22})\}\,U_1 - (2 - \tfrac{2}{3}\gamma)f', \\
T_{22}^{(1)} &\sim \{2(1-\gamma)\,A_{22} - \tfrac{2}{3}\gamma(A_{11} - A_{22})\}\,U_1 - (2 - \tfrac{2}{3}\gamma)f', \\
T_{33}^{(1)} &\sim -\tfrac{2}{3}\gamma(A_{11} - A_{22})\,U_1 - \tfrac{2}{3}\gamma f', \\
T_{12}^{(1)} &\sim -2(1-\gamma)\,(A_{11} + A_{22})f', \\
D_1 &\sim 0
\end{aligned}\right\} \quad (3.10)$$

as $Y \to \infty$.

The solutions (3.10) match with the outer-layer solutions, where the only forcing terms in the equations are the production and 'rapid' pressure terms throughout the layer.

We also require a lower boundary condition, which is obtained from the wall layer. At the outer edge of the wall layer, the stresses and dissipation satisfy the usual wall-layer equilibrium. Thus, with co-ordinates aligned with the local surface, the Reynolds-stress tensor is $\tau_w^+ A_{ij}$.

In order to match with the Reynolds-stress sublayer solution, this tensor must be rotated into the global co-ordinate axes which are aligned with the flat surface. After substituting the expansion for τ_w^+ and rotating, we find

$$\left.\begin{aligned}
T_{11}^{(1)} &\sim 2A_{11}U_1 - 2f', \\
T_{22}^{(1)} &\sim 2A_{22}U_1 + 2f', \\
T_{33}^{(1)} &\sim 2A_{33}U_1, \\
T_{12}^{(1)} &\sim 2U_1 + (A_{11} - A_{22})f', \\
D_1 &\sim 3U_1/\kappa Y
\end{aligned}\right\} \tag{3.11}$$

as $Y \to 0$.

The expression for D_1 arises from the wall-layer dissipation, which equals $(\tau_w^+)^{\frac{3}{2}}/\kappa y^+$ as $y^+ \to \infty$.

We now have a complete set of equations and boundary conditions for the determination of the first-order Reynolds-stress perturbations. We do not need to solve for U_3 since we only require $\partial U_3/\partial Y$ in equations (3.5)–(3.9). Differentiating (2.20) with respect to Y,

$$\frac{\partial}{\partial x}\left(\frac{\partial U_3}{\partial Y}\right) = f''' + \frac{\partial^2 T_{12}^{(1)}}{\partial Y^2} - \frac{1}{\kappa Y}\frac{\partial U_1}{dx}. \tag{3.12}$$

The full solution for U_3 requires the outer solution in order to determine P_3, and this is complicated since the boundary-layer profile, $u_{BL}(y)$ is involved. However, U_3 is a third-order perturbation and is not a significant contribution to any speed-up effects; our main interest is in the prediction of the Reynolds stresses, so we use (3.12) to eliminate u_3 from equations (3.5)–(3.9).

Although a Fourier transform in the x direction can be used to remove the x derivatives, equations (3.5)–(3.9) are too complicated to facilitate an analytic solution despite their linearity. Therefore the equations were solved numerically using a variable-step Kutta–Merson integration routine. Six independent solutions satisfying the lower boundary condition were integrated upward to some large value of Y, and then the linearity was exploited in order to calculate a linear combination which satisfied the upper boundary condition. This procedure could be followed for a number of Fourier modes to calculate the solution for a particular shape of hill, but in the next section we shall present the single Fourier solution only. The lower boundary condition cannot be applied at $Y = 0$ since there is a singularity on the surface, so it is applied at some small value $Y = Y_0$. The value of Y_0 was varied until it was sufficiently small for the results to be insensitive. The upper boundary was also varied in a similar fashion.

4. Results for sinusoidal topography

We shall present the Reynolds-stress perturbation results for flow over the lower surface
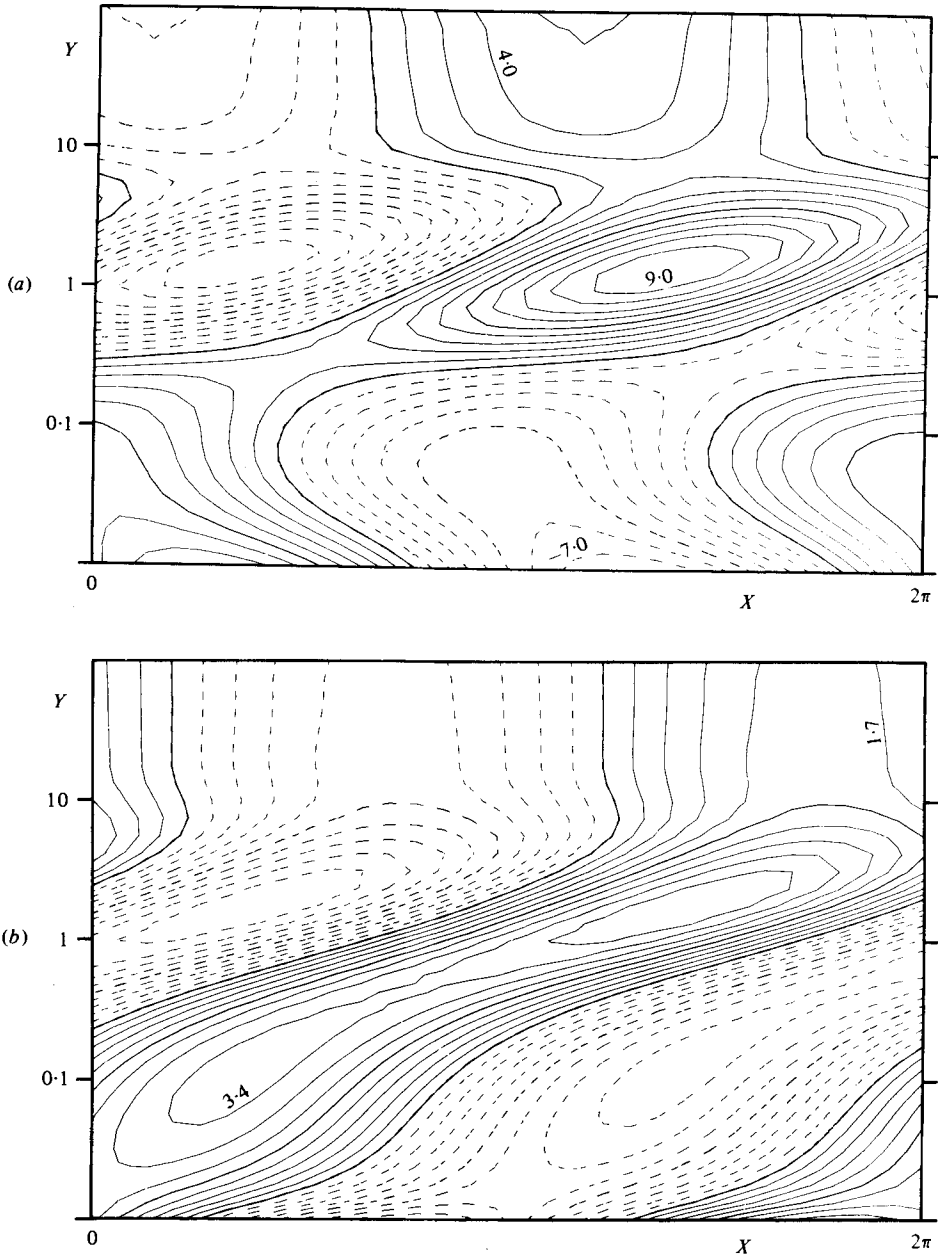
$$y = \epsilon^{\frac{1}{2}}\cos x. \tag{4.1}$$

FIGURE 2 (*a*, *b*). For legend see next page.

In fact, it can be easily shown that if the wavelength is L, rather than 2π, then the solutions are identical provided the amplitudes of the 'cos x solutions' are multiplied by $2\pi/L$, and the height scale is multiplied by $L/2\pi$. That is, a shorter wavelength produces a larger amplitude with a smaller vertical scale. In view of this scale-independence of the solution, and the lack of accurate experimental data for comparison, it was felt adequate to restrict the numerical solutions to the simple topography
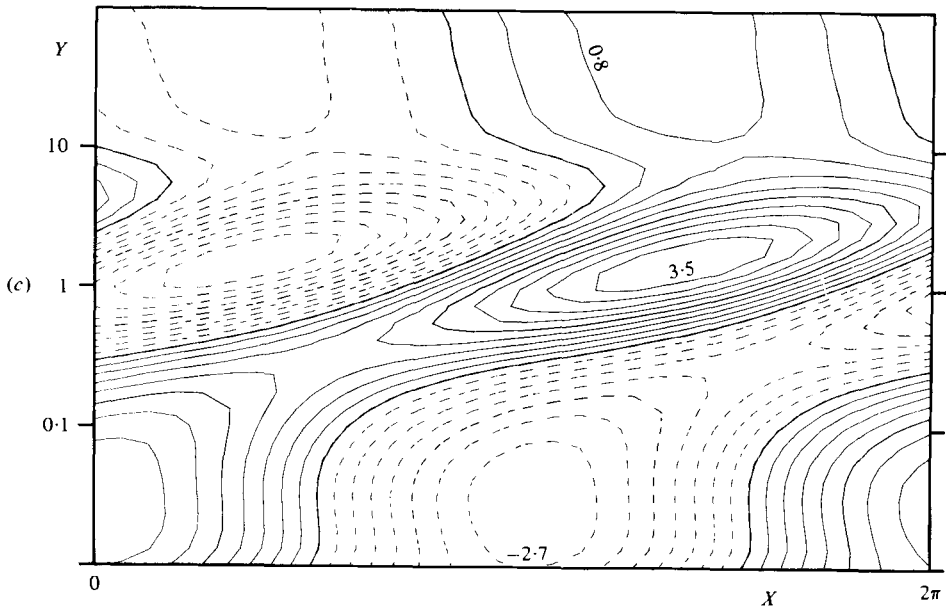
Figure 2. Normal Reynolds-stress perturbations in the Reynolds-stress sublayer for sinusoidal topography. Dashed contours denote a negative perturbation. (a) $\Delta\overline{(u^2)}/\epsilon^{\frac{5}{3}}U_0^2 = -T_{11}^{(1)}$, contour interval 1·0. (b) $\Delta\overline{(v^2)}/\epsilon^{\frac{5}{3}}U_0^2 = -T_{22}^{(1)}$, contour interval 0·43. (c) $\Delta\overline{(w^2)}/\epsilon^{\frac{5}{3}}U_0^2 = -T_{33}^{(1)}$, contour interval 0·38.

given by (4.1). This is particularly suitable for the Fourier transform method of solution which was described in the previous section.

In the solutions for the Reynolds stress variations presented below, the boundary conditions were applied at $Y = 0·01$ and $Y = 100$. These values were determined by trial and error to be sufficient for the application of the asymptotic conditions at these finite values not to affect the solution. We only present the Reynolds stress perturbations below, since the leading-order velocity and pressure perturbations are simply the well-known potential flow solutions.

Figure 2 illustrates the variations in the three components of the turbulence energy in the Reynolds-stress sublayer. It should be noted that this layer is thinner than the height of the surface variations, and lies along the curved surface. The trough of the wave lies in the centre of the domain. The equilibrium dimensionless surface-layer values of the turbulence energy components are derived from the second-order closure model as $(\overline{u^2}, \overline{v^2}, \overline{\omega^2}) = \epsilon^2 U_0^2(2·83, 1·35, 1·35) = \epsilon^2 U_0^2(A_{11}, A_{22}, A_{33})$. All three perturbation components show the anticipated singular variation near the surface; note the logarithmic vertical scale. The surface values are not identically in phase with the topography owing to the rotation of the Reynolds-stress tensor into the undisturbed Cartesian co-ordinate system. However, there is a general tendency for all three components to maximize in the neighbourhood of the peak and minimize in the trough, as would be expected from equilibrium layer arguments. The rapid-distortion variations are given by the asymptotic behaviour at large Y, and it will be seen that the streamwise component is reduced over the peak, whilst the normal component is increased; these changes have a similar magnitude to the theoretical rapid-distortion
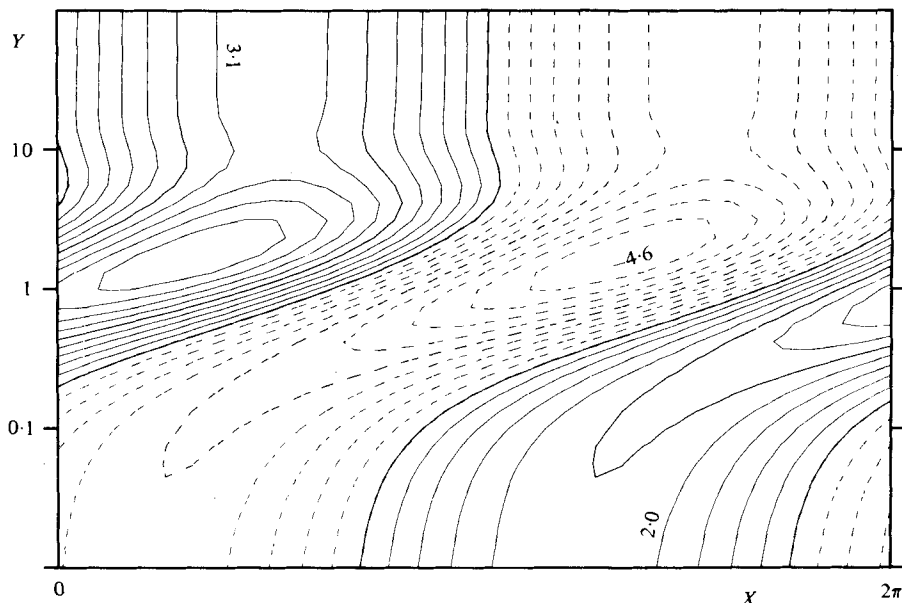
FIGURE 3. Reynolds-stress perturbation, $\Delta(\overline{uv})/\epsilon^{\frac{5}{2}} U_0^2 = -T_{12}^{(1)}$.
Contour interval 0·51.

results of Britter *et al.* (1980). Between these two limits there is a dramatic variation of the turbulence energy components. In general, there is a local maximum in the perturbation amplitude near $Y = 1$, and this maximum is roughly $180°$ out of phase with the surface variation. The amplitude of this elevated maximum is slightly larger than the surface-layer amplitude.

The perturbation stress component $\Delta(\overline{uv})/\epsilon^{\frac{5}{2}} U_0^2 = -T_{12}^{(1)}$ is plotted in figure 3, and shows the same general features as the normal components. As in figure 2, the minimum on the surface is slightly downstream of the peak of the topography owing to the rotation of the co-ordinates. The elevated maximum in the amplitude is also larger than the amplitude of the surface variation.

The structure displayed in these results is qualitatively similar to the numerical results of Taylor, Gent & Keen (1976) for turbulent flow over a wavy surface. They only consider the surface-layer flow since the horizontal wavelength is very short, therefore the quantitative values are not strictly comparable. In fact their numerical values are quite different; for example their elevated extrema have nearly the same amplitude as the surface extreme compared to a factor of two difference in figure 3. However, we shall show below in § 7 that stresses obtained under different closure assumptions will be completely different, therefore detailed comparisons are of limited value. The results of Taylor *et al.* are also nonlinear, but they confirm the very rapid variations of the Reynolds stress near the surface; this behaviour was deduced in the previous section independently of any closure assumption. It will also be shown below in §6 that the present theory is easily modified to accommodate shorter length scales of topography.

The magnitude of the perturbations in figures 2 and 3 is perhaps surprisingly large.

The topography (4.1) introduces a first-order dimensionless velocity perturbation of magnitude unity at the surface, but the relative changes in the Reynolds-stress components at the elevated maximum is roughly three to four times larger than the relative change in velocity. These changes in Reynolds stress seem the most promising possibility for comparison between experiment and theory; however it should be remembered that these variations are within a thin layer adjacent to the surface, and are very difficult to measure in wind-tunnel experiments with artificially roughened surfaces.

Townsend (1972) also calculates the Reynolds stresses using a closure at the same level as the current work. His prediction of the surface-stress variation is quite unlike our results (2.27) which is in phase with the wave. He obtains a similar magnitude but the phase difference is $O(1)$ as can be seen from Townsend's table 1. Since (2.27) is a very simple asymptotic result, the disagreement seems fundamental. A possible source of the discrepancy is Townsend's treatment of the lower boundary condition as expressed in his equations (3.5) and (3.6). This is a linearization of the lower boundary onto $y = 0$ ($z = 0$ in Townsend's notation) and effectively involves expanding in a Taylor series about a singular point in the logarithmic profile. The term h/Kz (Townsend's notation) in his equation (3.6) appears to invalidate the linearization procedure as $z \to 0$ but a more detailed analysis would be necessary to resolve the discrepancy properly.

5. Perturbation force on the lower boundary

As mentioned in §1, the change in total force on the lower boundary is of some interest. This force is composed of the change in stresses on the boundary which extend upstream and downstream of the obstacle, and also the pressure force which acts locally on the hump. The normal Reynolds stresses are somewhat arbitrarily counted in the first category here.

The total force is given by

$$F_i = \int (\tau_{ij} - p\delta_{ij}) n_j \, dl \tag{5.1}$$

where τ_{ij} is the stress tensor, p is the pressure, n_j is the unit normal to the surface, and the integration is calculated along the surface. We first calculate the drag contribution from the Reynolds-stress perturbations. The leading contribution can be shown to be

$$\frac{F_R}{\epsilon^2 U_0^2 \delta} = \int_{-\infty}^{\infty} \{T_{12}^{(2)}(x, 0) - f' T_{11}^{(1)}(x, 0)\} \, dx. \tag{5.2}$$

Now

$$T_{11}^{(1)}(x, 0) = 2A_{11} U_1 - 2f'$$

from (3.11), and taking the expansion to second order, we find

$$T_{12}^{(2)}(x, 0) = 2U_2 - f'^2 + U_1^2 + 2(A_{11} - A_{22})f' U_1.$$

Using the expressions for U_1 and U_2, i.e. (2.17), (2.18),

$$\frac{F_R}{\epsilon^2 U_0^2 \delta} = \int_{-\infty}^{\infty} (2u_2(x, 0) + 2ff'' + f'^2 + U_1^2 - 2A_{22}f' U_1) \, dx$$

$$= \int_{-\infty}^{\infty} (2u_2(x,0) + U_1^2 - f'^2) \, dx$$

since $\int_{-\infty}^{\infty} f' U_1 \, dx = 0$ where U_1 is the potential flow solution. For potential flow

$$\int_{-\infty}^{\infty} U_1^2 \, dx = \int_{-\infty}^{\infty} f'^2 \, dx,$$

therefore the only contribution comes from u_2. However, it is easy to show that

$$\int_{-\infty}^{\infty} u_2(x,0) \, dx = 0,$$

thus $F_R = 0$, and there is no contribution from the Reynolds stresses at this order.

The calculation of the pressure force is more difficult. We note that up to $O(\epsilon^{\frac{5}{4}})$ there are no terms influencing the pressure perturbation which involve the Reynolds stresses. The Reynolds stresses first appear in the outer-flow equations at $O(\epsilon^{\frac{5}{4}})$ whilst the displacement vertical velocity which provides the coupling between the outer layer and the sublayer first arises from equation (2.20), and is also $O(\epsilon^{\frac{5}{4}})$. All higher order vertical velocities at the outer edge of the Reynolds-stress sublayer vary like Y or $\ln Y$ and simply match with the inviscid flow in the outer layer with undisturbed profile $1 + \epsilon u_{\mathrm{BL}}(y)$. Since this flow, although rotational, is still inviscid there is no resultant force on the lower boundary. We have

$$V_3^* = -\int_0^Y \frac{\partial U_3}{\partial x} \, dY,$$

therefore using (2.20), the only $O(\epsilon^{\frac{5}{4}})$ contribution as $Y \to \infty$ comes from the stress gradient term, and if we denote this displacement contribution by V_{3d} then

$$V_{3d} = \lim_{Y \to \infty} [T_{12}^{(1)}(x,0) - T_{12}^{(1)}(x,Y)]$$

$$= 2U_1 + (A_{11} - A_{22})f' + 2(1-\gamma)(A_{11} + A_{12})f' \qquad (5.3)$$

using (3.10) and (3.11).

We emphasize that there are other terms in the lower boundary condition for the $O(\epsilon^{\frac{5}{4}})$ perturbation in the outer flow, but this is the only one which produces a force, and we can consider V_{3d} is isolation since the equations are linear.

The $O(\epsilon^{\frac{5}{4}})$ equations for the outer flow are

$$\left. \begin{aligned} \frac{\partial u_5}{\partial x} &= -\frac{\partial p_5}{\partial x} + \frac{\partial \tau_{11}^{(1)}}{\partial x} + \frac{\partial \tau_{12}^{(1)}}{\partial y} + N_x, \\[2mm] \frac{\partial v_5}{\partial x} &= -\frac{\partial p_5}{\partial y} + \frac{\partial \tau_{12}^{(1)}}{\partial x} + \frac{\partial \tau_{22}^{(1)}}{\partial y} + N_y, \\[2mm] \frac{\partial u_5}{\partial x} + \frac{\partial v_5}{\partial y} &= 0, \end{aligned} \right\} \qquad (5.4)$$

where $\tau_{ij}^{(1)}$ is the $O(\epsilon^{\frac{1}{4}})$ Reynolds-stress perturbation in the outer flow, and N_x, N_y represent the nonlinear interaction terms from the lower-order perturbation velocities. The lower boundary condition on (5.4) is

$$v_5 = V_{3d} + V_{\mathrm{inv}} \quad \text{on} \quad y = 0 \qquad (5.5)$$

where V_{inv} represents the vertical velocity contribution from the inviscid flow solution.

We define $u_5 = u_{1nv} + u_{5d}$, similarly for v_5, p_5 where

$$\left.\begin{aligned}
\frac{\partial u_{1nv}}{\partial x} &= -\frac{\partial p_{1nv}}{\partial x} + N_x, \quad \frac{\partial v_{1nv}}{\partial x} = -\frac{\partial p_{1nv}}{\partial y} + N_y, \\
\frac{\partial u_{1nv}}{\partial x} &+ \frac{\partial v_{1nv}}{\partial y} = 0, \quad v_{1nv} = V_{1nv} \quad \text{on} \quad y = 0.
\end{aligned}\right\} \tag{5.6}$$

Then

$$\left.\begin{aligned}
\frac{\partial u_{5d}}{\partial x} &= -\frac{\partial p_{5d}}{\partial x} + \frac{\partial \tau_{11}^{(1)}}{\partial x} + \frac{\partial \tau_{12}^{(1)}}{\partial y}, \\
\frac{\partial v_{5d}}{\partial x} &= -\frac{\partial p_{5d}}{\partial y} + \frac{\partial \tau_{12}^{(1)}}{\partial x} + \frac{\partial \tau_{22}^{(1)}}{\partial y}, \\
\frac{\partial u_{5d}}{\partial x} &+ \frac{\partial v_{5d}}{\partial y} = 0 \\
v_{5d} &= V_{3d} \quad \text{on} \quad y = 0.
\end{aligned}\right\} \tag{5.7}$$

and

Now since the problem (5.6) contains just the elements of the inviscid problem, there will be no force contribution from this; hence we only need to solve the problem (5.7).

Now the Reynolds-stress perturbations $\tau_{ij}^{(1)}$ are easily calculated from the rapid distortion limit of the second-order closure equations as

$$\left.\begin{aligned}
\tau_{11}^{(1)} &= -au_1 - bv_1, \\
\tau_{22}^{(1)} &= cu_1 - bv_1, \\
\tau_{12}^{(1)} &= -2(1-\gamma)(A_{11} + A_{22})v,
\end{aligned}\right\} \tag{5.8}$$

where

$$a = 2(1-\gamma)A_{11} + \tfrac{2}{3}\gamma(A_{11} - A_{22}),$$

$$b = 2 - \tfrac{2}{3}\gamma,$$

$$c = 2(1-\gamma)A_{22} - \tfrac{2}{3}\gamma(A_{11} - A_{22}).$$

Substituting (5.8) into (5.7), we obtain

$$\nabla^2 p_{5d} = 2(1-\gamma)(A_{11} + A_{22})\,\partial^2 u_1/\partial x^2. \tag{5.9}$$

Defining the Fourier transform $\tilde{u}(\omega, y) = \int_{-\infty}^{\infty} u(x, y)\,e^{-i\omega x}\,dx$, we obtain

$$\tilde{u}_1 = |\omega|\tilde{f}(\omega)\,e^{-|\omega|y},$$

therefore

$$\frac{\partial^2}{\partial y^2}\tilde{p}_{5d} - \omega^2 \tilde{p}_{5d} = -2(1-\gamma)(A_{11} + A_{22})\,\omega^2\,|\omega|\tilde{f}e^{-|\omega|y}. \tag{5.10}$$

Solving (5.10) with the lower boundary condition of (5.7), it can be shown that

$$\int_{-\infty}^{\infty} p_{5d}f'\,dx = \tfrac{2}{3}\gamma \int_{-\infty}^{\infty} f'^2\,dx. \tag{5.11}$$

However, this is not quite the pressure force on the boundary, since p_{5d} is the pressure at the outer edge of the Reynolds-stress sublayer. We have to calculate the $O(\epsilon^{\frac{1}{2}})$ pressure change across the inner layer. Now

$$-\frac{\partial P_5}{\partial Y} + \frac{\partial T_{22}^{(1)}}{\partial Y} = N_y \tag{5.12}$$

where N_y is a complicated set of inertial terms. It is quite straightforward to calculate N_y and to show that none of the terms produces an $O(1)$ change in P_5 across the layer, but the algebra is rather tedious and is therefore omitted. The result we require from (5.12) is that

$$P_{5d}(x, 0) = p_{5d}(x, 0) + \tau_{22}^{(1)}(x, 0) - T_{22}^{(1)}(x, 0)$$

where P_{5d} is the surface pressure responsible for the net force.

Thus

$$P_{5d} = p_{5d}(x, 0) + (2 - c) U_1 + (2 + b) f'$$

and therefore

$$\int_{-\infty}^{\infty} P_{5d} f' \, dx = \int_{-\infty}^{\infty} p_{5d} f' \, dx + (2 + b) \int_{-\infty}^{\infty} f'^2 \, dx$$

$$= 4 \int_{-\infty}^{\infty} f'^2 \, dx.$$

Hence the total pressure force, and also the total perturbation force on the boundary, is

$$F = 4\epsilon^3 U_0^2 \delta \int_{-\infty}^{\infty} f'^2 \, dx. \tag{5.13}$$

Note that the force due to the undisturbed boundary layer on a section of length δ is $F_0 = \epsilon^2 U_0^2 \delta$, and since the slope of the obstacle is $O(\epsilon^{\frac{1}{2}})$, the perturbation force is $O[(\text{slope})^2 \times F_0]$. Thus, although the perturbation pressures are very much larger, most of the pressure field produces no net force. It should be noted that the force in (5.13) does not depend on any empirical constants in the turbulence closure. It is also of interest that the force is sufficiently small for the pressure variation across the inner layer to be important.

The force result (5.13) does not really conflict with the result of Counihan *et al.* (1974) that there is zero net-force perturbation on the boundary. Their result stems from a momentum integral calculation over a control volume whose size is of too large a magnitude to obtain the result (5.13). The present result is of the same asymptotic magnitude as Townsend's (1972) calculation of the pressure force, although there is some discrepancy in the numerical value. (5.13) implies that the average perturbation stress on a wavy surface would be $2\alpha^2 u_*^2$, where α is the maximum wave step. Although Townsend considers a wavelength L much less than δ, we shall show in the next section that the modifications to the asymptotic theory are trivial. In this case, ϵ can be defined as $\kappa/\ln(L/y_0)$; Townsend computes the stress perturbation for ϵ between 0·05 and 0·033 and obtains results between $4\alpha^2 u_*^2$ and $5·5\alpha^2 u_*^2$. However, in view of the serious discrepancy between Townsend's stress predictions and the current work, we would not expect quantitative agreement between the forces. We shall return to the question of the force on the obstacle in §7 when the effects of different closure assumptions are examined.

6. Discussion

The analysis we have presented is not strictly limited to topography with a horizontal length scale of order δ; shorter humps are easily accommodated. If we consider an obstacle of length $O(\epsilon^n \delta)$, with $n \geq 0$, we define an outer layer of thickness $\epsilon^n \delta$ and a Reynolds-stress sublayer of thickness $\epsilon^{n+1} \delta$. The undisturbed profiles in the two layers will be

$$\frac{u}{U_0} = 1 + \frac{n\epsilon}{\kappa} \ln \epsilon + \epsilon u_{\mathrm{BL}}(y)$$

and

$$\frac{u}{U_0} = 1 + \frac{(n+1)\epsilon}{\kappa} \ln \epsilon + \epsilon U_{\mathrm{BL}}(Y)$$

respectively, where $u_{\mathrm{BL}}(y) \sim \ln y/\kappa$ and $U_{\mathrm{BL}}(Y) \sim \ln Y/\kappa$ as y, $Y \to 0$. Since the wall layer is transcendentally thin, these algebraic changes in outer-layer magnitudes have no effect on the lower boundary conditions. Thus, the equations will be identical apart from the coefficient of the $\epsilon \ln \epsilon$ perturbation, and the generation of logarithmic terms in the outer-layer expansion. The factor $n \ln \epsilon/\kappa$ can be absorbed into the definition of the free-stream velocity, which then leaves the equations unchanged but uses the boundary-layer velocity at height $O(\epsilon^n \delta)$ as the outer velocity scale. This wide range of applicability could have been anticipated from the observation in §4 that the form of the solution is independent of the length scale. Clearly in any actual case with a finite value of ϵ there will be some definite lower limit on the size of the hump.

The situation is more complicated with longer humps, since the outer layer becomes deeper than the boundary layer, and the boundary-layer scale must be retained as a middle layer for the higher-order perturbations. When the hump length is $O(\epsilon^{-1}\delta)$ or greater, then the Reynolds-stress sublayer merges into the main boundary layer and the equations are different since there is no rapid distortion region for the Reynolds stresses. On this length scale, the hump is much higher than the boundary layer, which is a thin region on the surface. For length scales much longer than $\epsilon^{-1}\delta$, the boundary layer is in local equilibrium with the potential flow to first order everywhere. We shall not explore the structure of these long humps in detail, because the scale already considered contains most of the essential features of the dynamics. In all cases, it seems that the slopes must be $O(1)$ in order to provoke separation.

In view of the similarity of the theoretical work of Jackson & Hunt (1975), its relationship to the present work will be examined. Jackson & Hunt consider only two layers; an outer layer where the flow is inviscid as in the present work, and an inner layer which bears some resemblance to our Reynolds-stress sublayer. There is some difficulty with the expansions, since they treat $\ln (l/y_0)$ and $\ln (L/y_0)$ as different large parameters in some senses, where l and L are the scales of the inner and outer layers respectively. However these quantities are both $O(\epsilon^{-1})$ in the notation of this paper, and they are in fact required to be the same in order for their velocity perturbations to match. Given that $\ln (l/y_0) = O(\epsilon^{-1})$, then $l/L = O(\epsilon)$ in Jackson & Hunt's theory, precisely as in the present work. However, a mixing length closure is assumed for their inner layer, which has been shown to be inadequate in §3 above. The final result of Jackson & Hunt is that the inner-layer velocity perturbation is the potential

flow solution at the surface plus a contribution from the Reynolds stresses in the form of a Bessel function. But the Bessel function contribution is relatively $O(1/\ln(l/y_0))$ which is of the same order as other neglected terms in the equation, hence the approximation is not strictly rational. However, it is worth examining their solution in the light of the present asymptotic theory.

One parameter of practical interest is the relative speed-up $\Delta s = \Delta u(x, y + h(x))/u_0(y)$ where $\Delta u(x, y + h)$ is the velocity perturbation at a point distance y above the surface $h(x)$ and $u_0(y)$ is the upstream profile. If the height of the hill is small enough for the nonlinear term U_2 in (2.12) to be smaller than the linear term U_3, i.e. $|\epsilon^{\frac{1}{2}}f| \ll \epsilon \ln \epsilon$ so that the obstacle is smaller than $O(\epsilon^{\frac{1}{2}}\delta)$, then the speed-up is easily seen to be $\Delta s = U_1(1 - 2\epsilon \ln \epsilon/\kappa)$ in the Reynolds stress sublayer, using (2.19). This is in agreement with Jackson & Hunt's equation (3.22). By continuing the expansion for the surface stress (2.25), it can be shown that Δs is unchanged in the wall layer, as is Jackson and Hunt's solution. Thus, although Jackson and Hunt's equations near the surface are not justified, their solution for the velocity perturbation is asymptotically correct throughout layer. This is perhaps reassuring in view of the reported successes of the theory in comparison with numerical results, Deaves (1975), and atmospheric observations, Mason & Sykes (1979b). In fact, Jackson & Hunt's prediction of Δs is perhaps usefully viewed as a uniformly valid combination of the wall layer and the Reynolds stress sublayer solutions since any practical application would necessitate joining the various asymptotic layers in some fashion.

The work of Knight (1977) shows a degree of overlap with the present theory; the thickness of the inner layer is the same, and the leading-order velocity perturbation is also the same. Knight employs a two-equation turbulence model of Saffman (1970), but still uses an effective viscosity to obtain the Reynolds stresses. His closure produces significantly different results as discussed in the next section but unfortunately there are insufficient details in his paper to make further comments.

7. Effects of different closures

It is of interest to note which features of the solution depend on the closure assumptions employed. We shall show that the stresses in the outer layer, and hence the pressure force on the surface, are very sensitive to the closure.

The theories of Jackson & Hunt (1973) and also of Knight (1977) show that the inner layer emerges quite naturally from various closure assumptions, with stresses of magnitude $O(\epsilon^{\frac{1}{2}}u_*^2)$ if we consider topography of slope $O(\epsilon^{\frac{1}{2}})$. The simplest closure assumption is probably the mixing length model as used by Jackson & Hunt. This gives the stress on the product of the square of a mixing length and the square of a velocity gradient. Thus, if this closure was applied in the outer flow, where the mixing length is $O(\delta)$ and the velocity gradient is $O(\epsilon^{\frac{1}{2}}U_0/\delta)$ we obtain a stress of $O(\epsilon U_0^2)$. The closures of Knight (1977) and Taylor (1977) employ transport equations for turbulence energy, but still use an effective viscosity to relate velocity gradients to the Reynolds stresses. It can be shown that the effective viscosity maintains its undisturbed magnitude of $O(u_*\delta)$ in the outer flow, hence the stresses are $O(\epsilon^{\frac{1}{2}}u_*U_0) = O(\epsilon^{\frac{1}{2}}U_0^2)$. These magnitudes are to be compared with the second-order closure and rapid-distortion results, which show that the perturbation stresses are $O(\epsilon^{\frac{1}{2}}U_0^2)$. It should be noted that the perturbation stresses from the other models are actually much larger than

	Pressure force from Taylor (1977)	Pressure force from (5.13)	Ratio of Taylor's force to analytic prediction
Short hill			
$a = 1000 y_0$ $b = 5000 y_0$	$7 \cdot 19 \times 10^3$	$1 \cdot 0 \times 10^3$	$7 \cdot 2$
Medium hill			
$a = 4000 y_0$ $b = 20\,000 y_0$	$2 \cdot 92 \times 10^4$	$4 \cdot 0 \times 10^4$	$7 \cdot 3$
Long hill			
$a = 10\,000 y_0$ $b = 50\,000 y_0$	$7 \cdot 13 \times 10^4$	$1 \cdot 0 \times 10^4$	$7 \cdot 1$

TABLE 1. Comparison between forces on Gaussian hills $h = a \exp(-(x/b)^2)$ from Taylor (1977) and prediction of (5.13).

the undisturbed stress. It is clear from this order-of-magnitude analysis that different closures will give completely different results for the stresses away from the surface, therefore detailed comparisons between various models are unlikely to be useful. The conclusion is that closures which do not allow for advection effects on the Reynolds stresses, but give a local relation between stress and velocity gradient, will give spuriously large Reynolds stresses in the outer flow.

These spurious Reynolds stresses are manifested in the pressure force on the lower boundary. As discussed in § 5, the perturbation pressure force arises at the order of the Reynolds stresses in the outer flow, since there is no interaction with the inner flow as in the laminar case. At lower orders we simply solve the inviscid equations of motion for flow over the topography, which gives no pressure force. Thus our results give a force of $O(\epsilon^3 U_0^2 \delta)$ but the mixing length model gives $O(\epsilon^{\frac{3}{2}} U_0^2 \delta)$ and the turbulent energy model gives $O(\epsilon^2 U_0^2 \delta)$. This is consistent with Knight's (1977) result that the phase of the pressure perturbation is $O(\epsilon)$ compared to the $O(\epsilon^2)$ prediction of the second-order closure theory.

Table 1 gives the pressure force results for three hills of different length from Taylor (1977). These are the form drags for the planetary boundary layer model with $\alpha_u = 0°$ from Taylor's table 1. Table 1 also gives the force on the hills calculated from (5.13), and the ratio of the two forces. We have shown that we would expect Taylor's result to be $O(\epsilon^{-1})$ larger than the current prediction, and although $\epsilon^{-1} = 30$ in this case, the ratios of about 7 are not inconsistent with this asymptotic result.

Townsend (1972) obtains a force of the same magnitude as the present work; this again results from his closure in the outer region which gives Reynolds stresses of the same order as the second-order closure in an asymptotic sense. The numerical value of the force depends on the details of the closure, but the important point is that the order of magnitude of the force is affected by the level of sophistication of the closure and that some form of Reynolds stress transport equations are required to obtain the correct asymptotic magnitude.

8. Summary and conclusions

We have presented a rational asymptotic theory of turbulent boundary-layer flow over a shallow hump, valid in the limit $\epsilon \to 0$ where ϵ is the ratio of the friction velocity to the free-stream speed. The flow structure consists of three layers; an outer layer on the scale of the boundary layer which is the same as the length of the obstacle; a Reynolds-stress sublayer which is a thin layer deformed along the surface of the obstacle; and a very thin wall layer adjacent to the surface. The structure is far less interactive than the laminar triple-deck, because of the very small velocity gradients in the outer part of a turbulent boundary layer. The leading-order velocity perturbations are simply the linearized potential flow solutions. The application of a second-order closure scheme to model the turbulent Reynolds stresses provides a description of the turbulence quantities, and allows a match between the equilibrium stresses near the surface and the rapidly distorted stresses in the outer flow. One feature worthy of note is the very large gradients in Reynolds stresses predicted near the surface, which implies that any numerical model of such flows must resolve variations on the scale of the surface roughness length or the viscous sublayer in the smooth-wall case.

The rational expansion schemes also permits the calculation of the net force perturbation on the obstacle. This drag is of the order of the force produced by the undisturbed flow on a section on a section of the surface of the same length as the obstacle multiplied by the square of the slope of the hump. The large, leading order pressure perturbations are governed by inviscid equations and produce no drag; this is in accord with the observed result that small surface variations do not produce large changes in net drag.

Examination of the consequences of various levels of turbulence closure has demonstrated that the Reynolds stresses in the outer layer, and also the pressure force on the hump, can take asymptotically different orders of magnitude. It has been shown that the correct magnitude is only obtained through a Reynolds-stress transport equation which allows some form of 'relaxation' of the Reynolds stresses, equivalent to a 'rapid-distortion' effect. Closures which relate the Reynolds stress to the local velocity gradient will result in spuriously large pressure forces.

It is hoped that this derivation of a rational asymptotic theory has clarified the dynamics of the flow, in particular the role of the Reynolds stresses. It should also be possible to apply this type of analysis to further problems involving turbulent boundary layer flow over obstacles, e.g. wind generation of water waves, or stably stratified flow.

REFERENCES

ADAMSON, T. C. & FEO, A. 1975 Interaction between a shock wave and a turbulent boundary layer in transonic flow. *SIAM J. of Appl. Math.* **29**, 121–145.

BATCHELOR, G. K. & PROUDMAN, I. 1954 The effect of rapid distortion of a fluid in turbulent motion. *Quart. J. Mech. Appl. Math.* **7**, 83–103.

BRADSHAW, P., FERRISS, D. H. & ATWELL, N. P. 1967 Calculation of boundary-layer development, using the turbulent energy equation. *J. Fluid Mech.* **28**, 593–616.

BRITTER, R. E., HUNT, J. C. R. & RICHARDS, K. J. 1980 Air flow over a two-dimensional hill: studies of velocity speed-up, roughness effects and turbulence. *Quart. J. Roy. Met. Soc.* (to appear).

COLES, D. 1956 The law of the wake in a turbulent boundary layer. *J. Fluid Mech.* **1**, 191–226.

COUNIHAN, J., HUNT, J. C. R. & JACKSON, P. S. 1974 Wakes behind two-dimensional surface obstacles in turbulent boundary layers. *J. Fluid Mech.* **64**, 529–563.

DEAVES, D. M. 1975 Wind over hills: a numerical approach. *J. Ind. Aerodynamics* **1**, 371–391.

DONALDSON, C. duP. 1971 A progress report on an attempt to construct an invariant model of model of turbulent shear flows. *Proc. AGARD Conf. on Turbulent Shear Flows, London*, paper B-1.

HANJALIC, K. & LAUNDER, B. E. 1972 A Reynolds stress model of turbulence and its application to thin shear flows. *J. Fluid Mech.* **52**, 609–638.

HINZE, J. O. 1959 *Turbulence.* McGraw-Hill.

HUNT, J. C. R. 1971 A theory for the laminar wake of a two-dimensional body in a boundary layer. *J. Fluid Mech.* **49**, 159–178.

IRWIN, H. P. A. H. & SMITH, P. A. 1975 Prediction of the effect of streamline curvature on turbulence. *Phys. Fluids* **18**, 624–630.

JACKSON, P. S. & HUNT, J. C. R. 1975 Turbulent wind flow over a low hill. *Quart. J. Roy. Met. Soc.* **101**, 929–955.

KNIGHT, D. 1977 Turbulent flow over a wavy boundary. *Boundary Layer Met.* **11**, 205–222.

LAUNDER, B. E., REECE, G. J. & RODI, W. 1975 Progress in the development of a Reynolds-stress turbulence closure. *J. Fluid Mech.* **68**, 537–566.

MASON, P. J. & SYKES, R. I. 1979a Separation effects in Ekman-layer flow over ridges. *Quart. J. Roy. Met. Soc.* **105**, 129–146.

MASON, P. J. & SYKES, R. I. 1979b Flow over an isolated hill of moderate slope. *Quart. J. Roy. Met. Soc.* **105**, 383–395.

MELLOR, G. L. 1972 The large Reynolds number asymptotic theory of turbulent boundary layers. *Int. J. Engng Sci.* **10**, 851–873.

MELNIK, R. E. & CHOW, R. 1975 Asymptotic theory of two-dimensional trailing edge flows. *Grunman Res. Dept. Rep.* RE-510.

MELNIK, R. E. & GROSSMAN, B. 1974 Analysis of the interaction between a weak normal shock wave with a turbulent boundary layer. *A.I.A.A. Paper* 74–598.

ROTTA, J. C. 1951 Statistische Theorie nichthomogener Turbulenz. *Z. Phys.* **129**, 547–572.

SAFFMAN, P. G. 1970 A model for inhomogeneous turbulent flow. *Proc. Roy. Soc.* A **317**, 417–433.

SMITH, F. T. 1973 Laminar flow over a small hump on a flat plate. *J. Fluid Mech.* **57**, 803–824.

SMITH, F. T., SYKES, R. I. & BRIGHTON, P. W. M. 1977 A two-dimensional boundary layer encountering a three-dimensional hump. *J. Fluid Mech.* **83**, 163–176.

STEWARTSON, K. 1974 Multistructured boundary layers on flat plates and related bodies. *Adv. Appl. Math.* **14**, 145–239.

SYKES, R. I. 1978 Stratification effects in boundary-layer flow over hills. *Proc. Roy. Soc.* A **361**, 225–243.

TAYLOR, P. A. 1977 Numerical studies of neutrally stratified planetary boundary layer flow above gentle topography. I. two-dimensional cases. *Boundary Layer Met.* **12**, 37–60.

TAYLOR, P. A. & GENT, P. R. 1974 A model of atmospheric boundary layer flow above an isolated two-dimensional 'hill'; an example of flow above gentle topography. *Boundary Layer Met.* **7**, 349–362.

TAYLOR, P. A., GENT, P. R. & KEEN, J. M. 1976 Some numerical solutions for turbulent boundary-layer flow above fixed, rough, wavy surfaces. *Geophys. J. R. Astronomical Soc.* **44**, 177–201.

TOWNSEND, A. A. 1972 Flow in a deep turbulent boundary layer over a surface distorted by water waves. *J. Fluid Mech.* **55**, 719–735.

YAJNIK, K. 1970 Asymptotic theory of turbulent shear flows. *J. Fluid Mech.* **42**, 411–427.